e-ISSN: 2146 - 9067

International Journal of Automotive Engineering and Technologies

journal homepage:

https://dergipark.org.tr/en/pub/ijaet

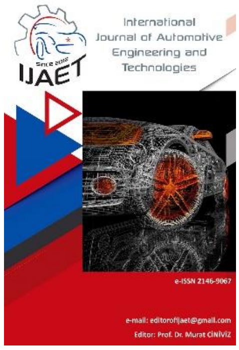

Original Research Article

hosted by Turkish JournalPark ACADEMIC

External torque sensor design providing wireless and real-time data customized for drivetrain

Sedat Tarakçı[1,*], Oğuzhan Aldemir[2], Turan Solmaz[3], Efe Işık[4]

[1,2,3,4] Tirsan Kardan A.S, Tirsan Kardan R&D Center, Manisa, Turkey.
[1] İzmir Institute of Technology, Department of Mechanical Engineering, İzmir, Turkey.

ARTICLE INFO

Orcid Numbers
1. 0000-0002-9125-5919
2. 0000-0002-3471-5034
3. 0000-0001-9166-9241
4. 0000-0001-7657-317X

Doi: 10.18245ijaet.982530

* Corresponding author
s.tarakci@tirsankardan.com.tr

Received: Aug 13, 2021
Accepted: Apr 14, 2022
Published: 01 May 2022
Published by Editorial Board Members of IJAET

ABSTRACT

In this study, a torque sensor design that can be used in both laboratory and field tests simulating road conditions of drivetrain of the vehicles is explained. Mechanical design of the sensor has been carried out via finite element method (FEM). Material of the torque sensor and the relevant heat treatment were determined. Electronic measurement circuit design and its setup have been carried out including amplifier, filter, ADC and data transmission features which are suited for full bridge connection. Verification and calibration tests have been performed with respect to DIN-51309. As a result of the studies, it was determined that the measurement accuracy of the system in the torque range of 250 ÷ 2500 Nm was 0.5%. The effect of noise-induced deviations was found 0.05% for the precision value. Consequently, a verified universal torque sensor has been developed for any drivetrain application under torsional effect with the given specifications. It is hoped that this sensor might become a common feature on any and every drivetrain for advanced monitoring of the drive components.

Keywords: Torque, driveshaft, data acquisition, calibration

1. Introduction

Automotive industry has increasingly become more of a sensing and measurement venue. Cars are turning into sensing and computing platforms. Naturally, more of the automotive components are interconnected, and hence communicating with both on-board computers and the drivers. These interconnected vehicle components are being easily monitored over their streamed data on statistics, health monitoring, tracking etc basis [1].

As computer controlled car systems have gained importance, different sensors have an important role of providing information on the controllers. Although, the sensor numbers are getting higher and automotive sensors continue to grow, torque sensors have still limited usage [2]. Torque sensor is a device to measure the torque on a rotating system [3]. Driveshaft and other drivetrain members are one of the measurement interest for torque sensors.

Main reasons for torque measurement are to control mechanical power for industrial reasons and to improve design studies. Engineering measurements play a significant role in the product development process. Examining the parts that make up the vehicle both provides information about product performance and provides input for future designs.

Drivetrain members are subjected to verification tests prior to design release [4]. Torque is one of the important variable that is measured in order to understand the limits of the product. This knowledge provides an opportunity to characterize the mechanical limits of the product [5].

A driveshaft may be overdesigned or selected improperly according to the type of vehicle. This situation affects driveshaft's costs and vehicle's weight in negative manner. An opportunity to collect data of transmitted torque of the driveshaft gives a chance to improve the design or to choose a suitable product [6].

As with all parts on the vehicle, the power transmission parts are also open to development. Power transmission parts are labored depending on the vehicle's transmission gear ratio, road conditions or vehicle trailer load. The said stresses are observed as a high torque effect on these parts. At this point, the monitoring of the torque effect emerges as a necessity during the operation in order to ensure appropriate and acceptable design.

Within the scope of this need, a study by [Joel C. Schnackenberg under the name of "Wheel Load Transducer"] is a torque measurement research. In the study carried out in 2002, the power transmission is made with the help of an adapter connected to the vehicle wheel hub. Thanks to this adapter, forces coming from different directions to the wheel hub are detected with the help of beams designed on different axes on the adapter [7].

Werner Nold's 2002 patent study "Recorder for Measuring applied forces has a rotationally symmetric body with measurement legs arranged between holes on which strain gages are placed to measured shear forces, which are intensitive to load placement" The mechanical system, which is symmetrically connected, designed to measure at the same time, and the mechanical system consisting of specially designed measuring points and directions are shown. In this study, forces in different axes are detected and recorded [8].

In the patent study titled "Torque Sensor Having Sealing Membrance" by Michael Grandl et al. in 2017, the basic torque measurement body and an inner flange design with the force input are made. Attenuated mounting sections are designed for sensors that generate output signals in mechanical design. In addition, sealing work has been done for this force measuring element so that it can work in the outdoor environment [9].

Niedworok presents an innovative approach to measure and monitor the dynamic torque changes in drive systems of the vehicles during their natural operation [10].

Sanponpute et al. designed a torque measuring device by using a loadcell. They verified their study by finite element analysis and experimental results [11].

In this study, a torque sensor design that can provide input for the development processes of drivetrains in vehicles, can be used in tests simulating road conditions, and collects torque data in fixed or rotating positions is explained. The sensor, which is the subject of this study, is designed to be resistant to external effects and impermeable to use in road conditions. Torque data collected by the sensor in real time can be read wirelessly by mobile devices or computer.

2. Mechanical Design

Torque is one of most important physical parameter for the drivetrain. The power transmission capacity of the drivetrain depends on the torque that can be transmitted. Therefore, design of driveshaft is done according to the capacity of torque. When torque is applied, tension occurs on the driveshaft and the resulting stress determines the capacity of driveshaft [12]. If the applied torque is out of the limits, the driveshaft may be damaged. If the torque is kept applying, that influences the product life [13].

The stress is calculated as follows.

$$\tau_{max} = \frac{\mathrm{TR}}{\mathrm{J}} \tag{1}$$

$$\mathrm{J} = \frac{\pi d^4}{32} \tag{2}$$

As shown in Figure 1 when the torque T apply to a bar, twisting occurs and angle of twist (θ) can be calculated by equation (3) [14, 15].

$$\theta = \frac{\mathrm{TL}}{\mathrm{J}} \tag{3}$$

Metallic materials are flexible according to their working principle. When the torque is applied metallic material, elastic strain is occurred. Strain gauges can measure amount of strain on the metallic material so stress can be calculated. In this case, if the torque is applied to a cylindrical geometry, amount of stress and torque can be calculated.

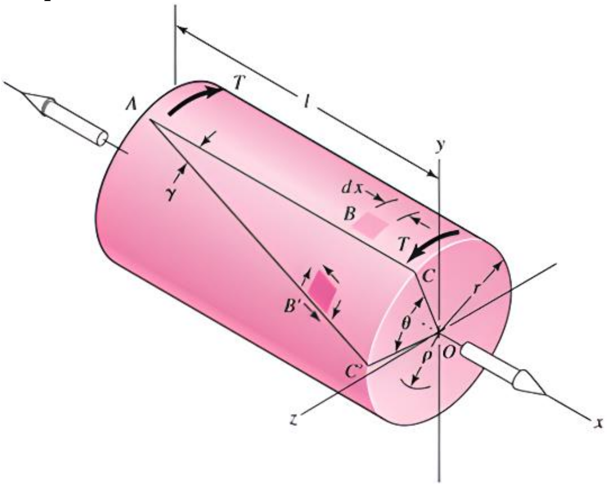

Figure 1. Torque applied to a bar [15]

When a rod is pulled, an elongation of ΔA occurs. Thus, L extends from its original length to L+ΔL.

The ratio of this elongation (or shortening) ΔL to the original length L is called strain and is denoted by the sign ε (epsilon) [16]. Figure 2 shows an elongated rod.

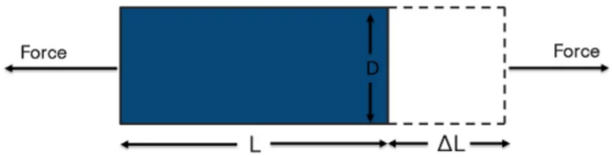

Figure 2. Rod under deformation [16]

When torque is applied to cylindrical geometry, as like in figure 3, a homogeneous field of orthogonal stresses is occurred. The stress can calculate the following formula [17].

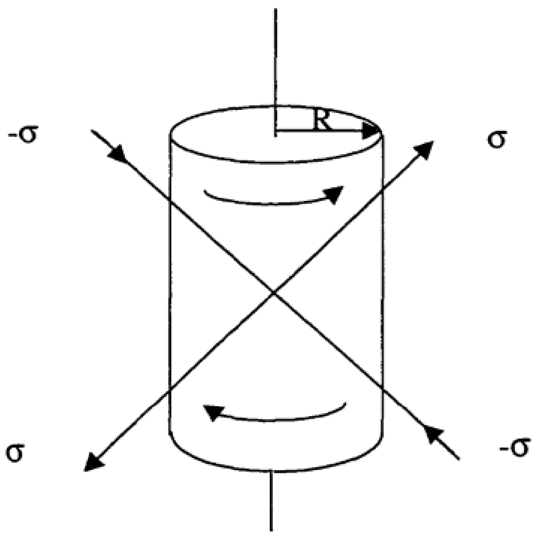

Figure 3. Stress distribution [3]

$$\sigma = \frac{2\tau r}{\pi R^4} \quad (4)$$

Since the strain gage measures the change between two points, the strain gage is attached to the circular surfaces as follows [3].

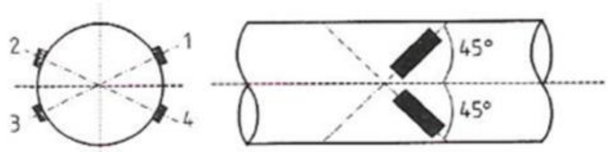

Figure 4. Strain gage application [17]

The purpose of the torque sensor is to measure torque over torque-transmitting parts such as the driveshaft. The measurement is taken by adhering strain gages to the torque sensor. At the same time, this sensor can be mounted to the component to be measured and the torque of that component can be measured. The geometry of the part to be measured is designed according to the strain gage working mechanism. Strain gage measurement mechanism for torque measurement is the formation of minus and plus orthogonal stress distribution as in figure 3. The orthogonal stress distribution should be as in Figure 5. As indicated in Figure 4, measurement is taken by connecting strain gages. The geometry of the part to be measured is designed to obtain a stress distribution like in figure 3.

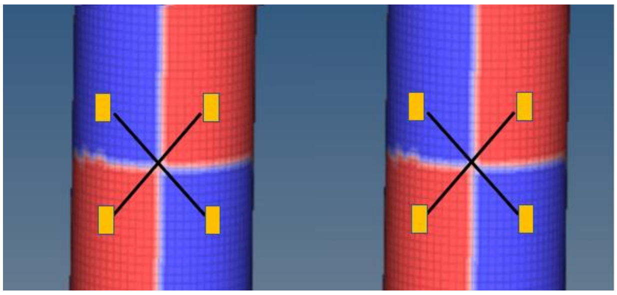

Figure 5. Orthogonal stress distribution on a pipe

Design& finite element analysis (FEA) studies were continued until desired stress distribution has been obtained. The part in figure 6 was designed according to further design & analysis studies. The analysis results show in figure 7 that stress distribution is similar to the desired one and homogeneous stress distribution was obtained.

According to the finite element results, the design in figure 6 was chosen. The maximum stress values that will occur on the part under the nominal torque are limited to 30% of the tensile strength of the part and the part dimensions have been determined accordingly the design analysis cycle.

4340 materials were selected to produce the design. According to ISO 18265, the hardness value was selected according to the desired tensile strength from the conversion table for low alloy steels [18]. The selected hardness value was measured as in figure 8 by taking a section from the heat treated geometry. The resultant hardness value was between HRC 34 to 35.

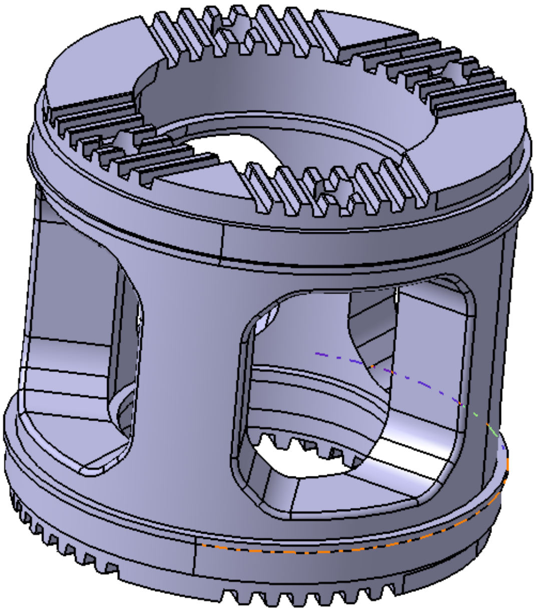

Figure 6. Final design of torque sensor

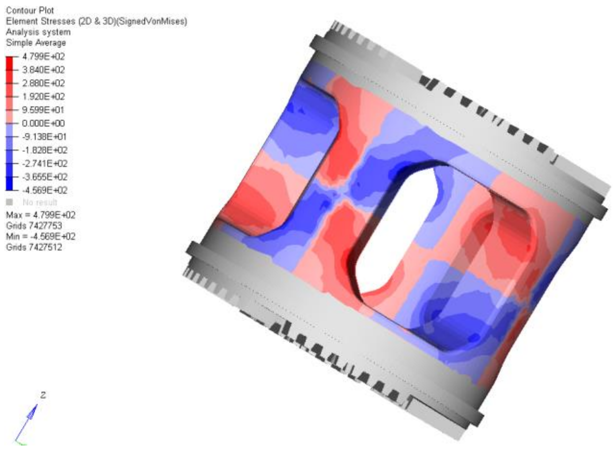

Figure 7. FEA results

Figure 8. Hardness measurement after heat treatment

3. Electronic Design

Suitable mechanical design has been completed for observing the strain flows clearly. In order to measure the torque data, strain gauge positioning have to be on strain flows direction. For this reason, strain gauges were placed at 45 degrees to the axis of the mechanical design part and 90 degrees between themselves. The locations and axial positions were determined and marked before to make the instrumentation correct. Figure 9 shows the electronic application of strain gages.

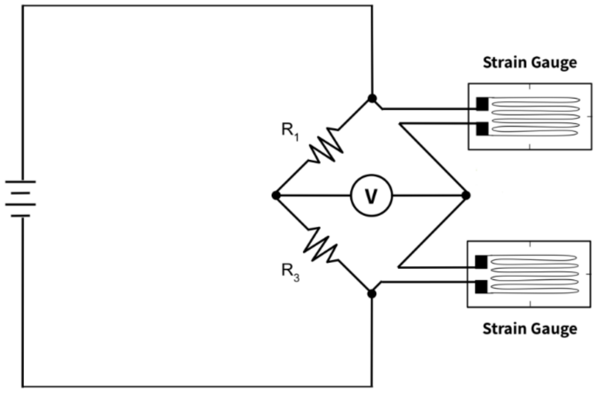

Figure 9. Half bridge application [19]

A printed circuit was designed for half bridge measurement method. Half bridge application includes two single strain gauge for torque measurement. There are two 1000 Ohm resistors parallel to strain gauges on the PCB. Resistors will be a reference for strain gauges and there will occur potential voltage difference [20]. This voltage is a very low level signal. The signal is amplified by a commercial amplifier before signal processing. Amplified signal is processed on the microcontroller and converted into a digital signal [21]. Digital signals, which are interpreted by mathematical operations on the microcontroller, are transferred to the wireless communication section of the PCB. Wirelessly broadcast data is made available to communication devices such as hand terminals, smart phones, tablets or computers. Bluetooth communication method was used to transmit data. A bluetooth module which uses SPP (serial port profile) was choosen. SPP imitates the RS232 serial connection and is used to send and receive data between two devices [22]. In the circuit diagram, the microcontroller supplied digital data from its TX port to the RX port of the bluetooth module. Transmitted data is broadcasted wirelessly.

The PCB's schematic and printing design was made on Proteus Professional software. Printing design and prototype of PCB is shown the figure 10. The 50 mW power required by the PCB is provided by lithium-ion batteries.

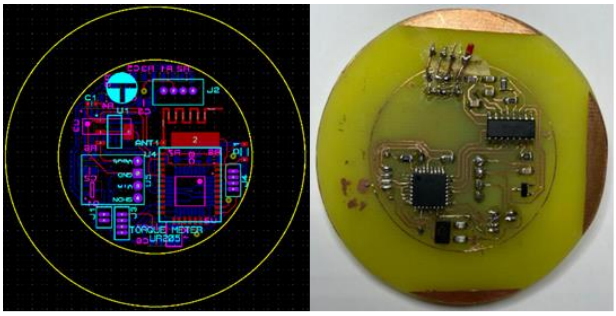

Figure 10. PCB design and prototype

The resistance of strain gage changes depending on the length of conductive wires inside the strain gauge. The change of the resistance affects the voltage of branches and creates a potential voltage difference. In the half bridge method described, the values of the 1000 ohm resistors were used as a reference. For this reason, the voltage difference is quite narrow and contains noises [21].

Full bridge method was applied as second approach to torque measurement. Here, decreasing the noise from collected data and to improve the sensitivity were aimed [23]. Two strain gauges of the same ohm value with reference resistors were used instead reference resistors used in half bridge method. Resistors, holes and paths on the PCB were updated and it has been suited for full bridge application.

A more stable signal was obtained with the full bridge application. The processes followed by the new generated signal are the same as the half bridge method. However, the sensitive voltage difference created by the full bridge changes the noise levels of the collected data. In figure 11, the measurement results obtained with full bridge and half bridge methods. It was clearly seen that the full bridge was more stable with low noise level.

4. Verification Tests

The Torque sensor, which is developed for calibration and verification tasks, has been subjected to a branch of tests according to a verification plan. DIN 51309 standard was used as a reference [24].

The torque sensor is mounted between the driveshaft and the test rig. In accordance with the full bridge connection, four strain gages have been glued on the driveshaft axis at 45° angle. Connections with electronic circuit have been carried out. The test setup is shown in Figure 12.

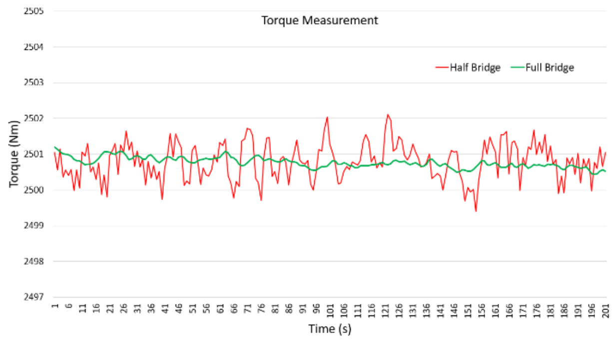

Figure 11. Comparison graph difference between half and full bridge

Figure 12. Test setup

Similarly, to the symmetry of the region where the strain gages had been applied in the torque sensor, a new set of strain gages were adhered and prepared for data collection with verified & calibrated commercial data acquisition board. The application can be seen in figure 13.

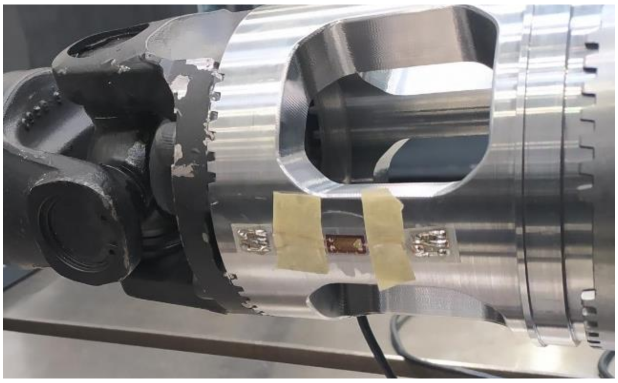

Figure 13. Strain gages dedicated for commercial board

According to the test plan, the system was preloaded 3 times and then let the system has been stabilized. Afterwards, calibration has been started. Torque level was gradually increased from 0 to 2500 Nm for 500 Nm steps in clockwise direction. The value read from the sensor has been recorded at each step. Afterwards, torque was applied in counter clockwise direction from 0 to 2500 Nm for 500 Nm steps. Applied torque values and the raw values read from the sensor are given in Table 1.

Table 1 Calibration values

Applied Torque (Nm)	**Sensor Data (Unit less)**
-2500	9611500
-2000	9240500
-1500	8868250
-1000	8495250
-500	8122250
0	7748500
500	7374750
1000	7001750
1500	6629000
2000	6257500
2500	5872500

When a graph was drawn with these values, information such as the equation and linearity of the curve has been obtained. In the graph shown in Figure 14, it is seen that the second order term is very small and negligible, and the calibration curve is linear.

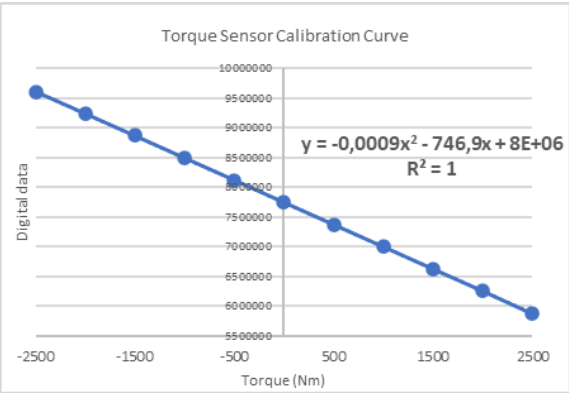

Figure 14. Calibration graph

The torque sensor has been calibrated by introducing the sensor data obtained during the calibration procedure to the developed software. A linear equation is defined for calibration between each calibration interval.

Even though figure 14 shows that a curve with high linearity is achieved in calibration procedure, calibration equations are constituted between each applied torque intervals. The fact that the torque sensor software allows to be defined calibration equation from multiple points increases the system accuracy and minimizes the problems related to linearity. Calibration formula is given in equation (5).

$$T_r = \frac{s - S_{ri}}{(S_{r(i+1)} - S_{ri}) \div (T_{a(i+1)} - T_{ai})} \quad (5)$$

$$for\ i = 1\ to\ n, n \in Z^+$$

Similarly, the calibration of the torque sensor was also performed with the strain gages associated with commercial data acquisition board. In Table 2 the applied torque values and related voltage values can be seen.

Table 2 Calibration values of commercial system

Applied Torque (Nm)	**Calibration values (mV/V)**
-2500	1.421
-2000	1.179
-1500	0.933
-1000	0.675
-500	0.409
0	0.152
500	-0.121
1000	-0.383
1500	-0.644
2000	-0.894
2500	-1.139

A graph was drawn with the collected values and information such as the equation and linearity of the curve has been obtained. In the graph shown in Figure 15, it is seen that the second order term is very small and negligible, and the calibration curve is linear.

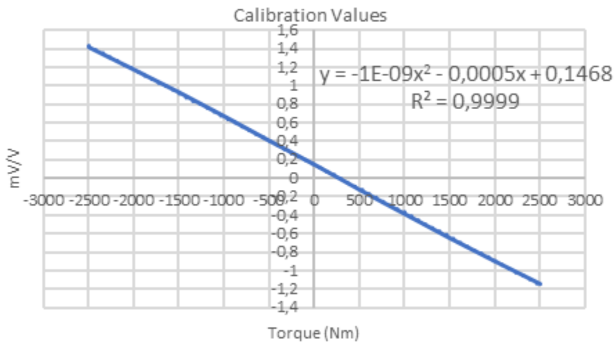

Figure 15. Calibration graph of commercial system

After the calibration, verification tests were started. In the validation tests, intermediate steps are also added. According to the test scenario, torque level was gradually increased from 0 to 2500 Nm for 250 Nm steps in clockwise direction. There are very short delays between steps regarding the continuous procedure [24]. It was also observed that the sensor was stabilized quickly. After reaching the value of 2500 Nm, it was decreased to 0 Nm with 250 Nm steps. Afterwards, 250 Nm steps were taken up to 2500 Nm in counterclockwise direction. After reaching 2500 Nm, it has been decreased to 0 again with 250 Nm steps. Collected data from the sensor during the test is shown in figure 16.

Simultaneously, torque verification tests have been performed with commercial system with the strain gages attached to the symmetrical arms of the sensor. The collected data from both systems were compared. Difference between the value read from the sensor and the applied torque value were compared according to equation (6) for each point.

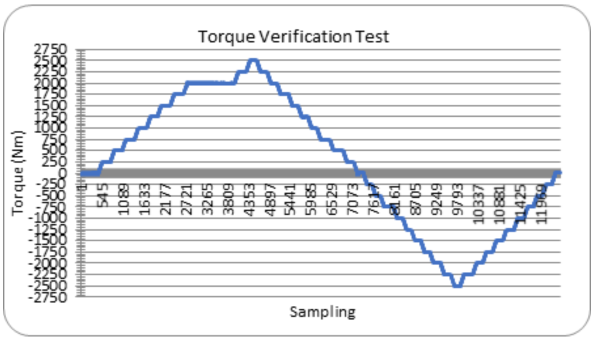

Figure 16. Torque sensor verification test

$$\%accuracy = \frac{T_{ri}-T_{ai}}{T_{ai}}x100 \qquad (6)$$
$$for\ i = 1\ to\ n, n \in\ Z^+$$

It is seen that there is a deviation of less than 0.5% between them.

Precision of the sensor was calculated for full bridge strain gage arrangement. A specific torque value was applied for a certain time period. The applied torque value was compared with the highest and the lowest value read by the sensor for that time interval. The ratio provides the precision level of the sensor. The deviation is caused by noise-induced effects. Figure 11 shows the deviations of the sensor for a limited time period. Equation (7) represents the approach to calculate the noise level. The effect of noise-induced deviations was found 0.05%.

$$\%precision = \frac{T_{r,max}-T_{r,min}}{T_{ai}}x100 \qquad (7)$$
$$for\ i = 1\ to\ n, n \in\ Z^+$$

The graph of the data collected by the commercial system is given in figure 17. Since the data acquisition frequencies of the commercial system and the system developed within the scope of this study are different from each other, the x-axis of the graph cannot be unified and both data cannot be shown in the same graph.

As a result, a comparison and verification study has been carried out both with the system developed within this study, with a commercial system and with the torque values applied by the verified test device. Figure 18 shows that data was read from all three systems simultaneously during the test.

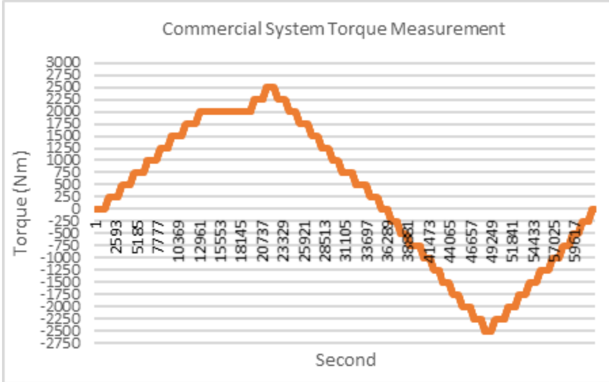

Figure 17. Torque measurement with commercial system verification test

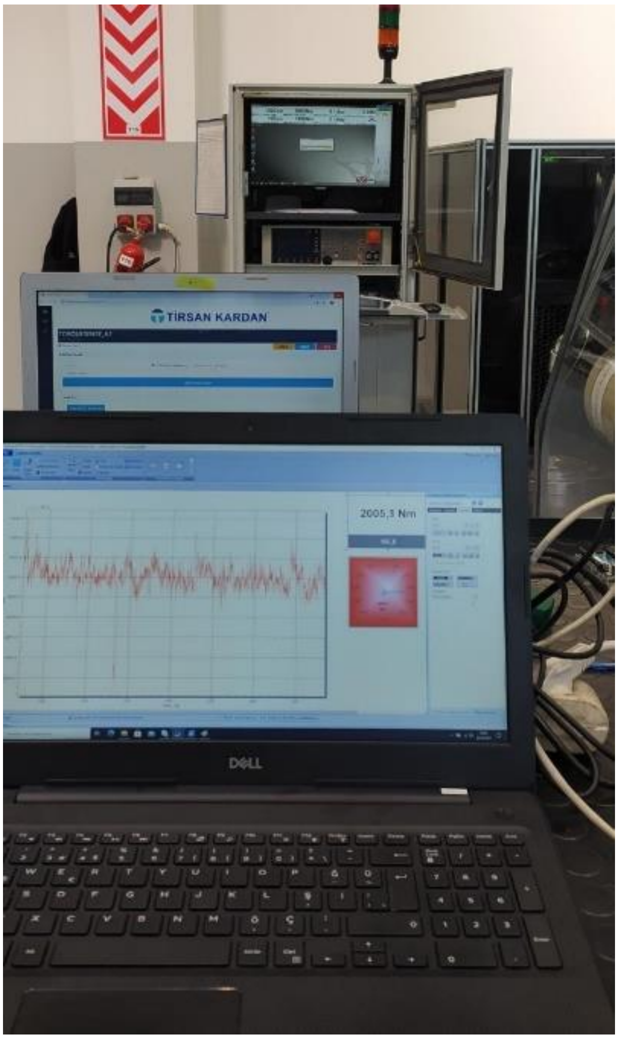

Figure 18. Test conditions

When the verification tests were completed, a validation test was also performed for the design & FEA cycle of the system. A test has been performed to determine the stress distribution and stress levels in order to understand relation between the FE analyzes and the real conditions and to determine the strength level of the torque sensor. A strain gage was attached to a suitable point on the sensor to collect strain data. Figure

19 shows the application.

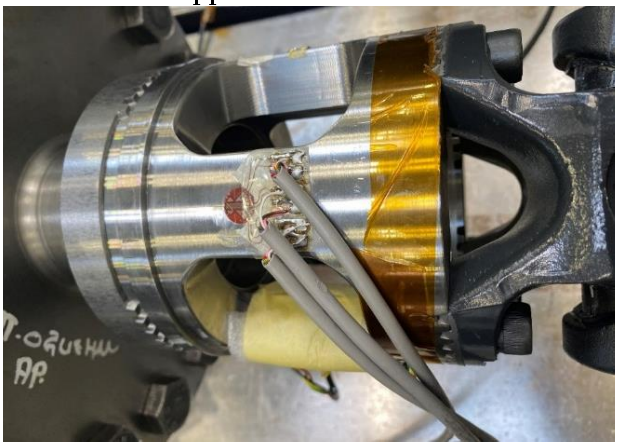

Figure 19. Design validation test

From this point, strain data were collected again with a commercial system. Torque was applied up to 3500 Nm both clockwise and counterclockwise with gradual increments. The collected strain values were converted into equivalent stress values and given in figure 20.

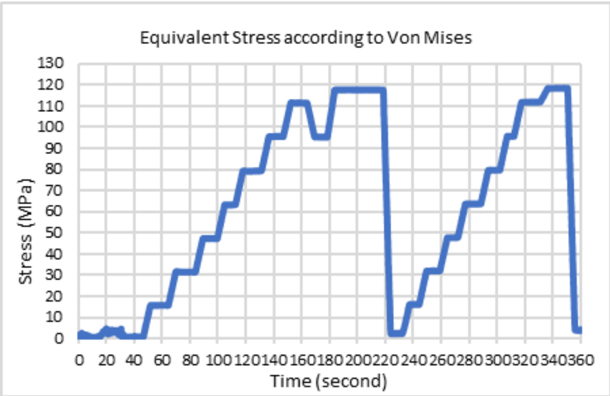

Figure 20. Equivalent stress graph

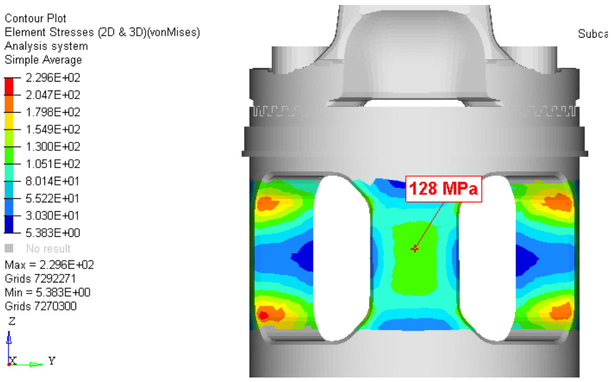

Figure 21. Finite element results of the torque sensor

When the collected data were examined, the stress value of the region where the strain gage was attached was measured as 118 MPa at a torque of 3500 Nm.

The region where the strain gage was attached was determined on the finite element model. The stress occurred at this point under the torque of 3500 Nm has been figured out on the model. The information about the model is given in figure 21.

The stress value of the region where the strain gage was attached was found as 128 MPa at a torque of 3500 Nm in the finite element model. When the two models were compared, deviation of 8% has been seen.

5.Conclusion

Prototype of the developed torque sensor has been produced regarding to design and analysis studies. Likewise, related electronic circuit design and production has been carried out. It was observed that accuracy errors and noise levels decreased with the full bridge application. The fact that the torque sensor software allows to be defined calibration equation from multiple points increases the system accuracy and minimizes the problems related to linearity. Calibration of the sensor has been performed on a test device which is calibrated in an accredited institution. In the subsequent verification tests, the accuracy of the system was demonstrated by comparing the measurements performed with the developed system both with the test rig and with a commercial system simultaneously.

The measurement accuracy of the system in the torque range of 250 ÷ 2500 Nm was calculated as 0.5%. The effect of noise-induced deviations was found 0.05% as the precision value.

In the test carried out for the design validation of the system, it was determined that there was an 8% deviation between the finite element model and the prototype. The model was considered suitable as it was within the 10% margin of error accepted for the finite element method.

Consequently, a verified torque sensor has been developed for any application under torsional effect with the given specifications.

Acknowledgement

We would like to acknowledge the support provided by Tirsan Kardan R & D center and test center during our experimental work.

CRediT authorship contribution statement

Sedat Tarakçı: Conceptualization, methodology, writing-original draft, validation, investigation, formal analysis, Project administration. **Oğuzhan Aldemir:** Validation, writing- original draft, Data Curation. **Turan Solmaz:** Methodology, investigation. **Efe Işık:**

conceptualization, supervision, Writing - Review & Editing

Declaration of Competing Interest

The authors declare that they have no known competing financial interests or personal relationships that could have appeared to influence the work reported in this paper.

Nomenclature

τ_{max} Maximum shear stress
T Torque
R Radius
J Polar moment of inertia
L Length
σ Normal Stress

6. References

1. O. Aldemir, S. Tarakçı, T. Solmaz, E. Işık, "External system design for real time monitoring of temperature and torque data on the driveshaft", 10th International Automotive Technologies Congress Book, 769-776, 2020.
2. G. Persson, O. Persson," Torque Sensor for Automotive Applications", Lund University, 2015.
3. M. Hilal Muftah, S. Mohamed Haris, K. Petroczki and E. Awad Khidir, "An Improved Strain Gauge-Based Dynamic Torque Measurement Method", International Journal of Circuits, Systems and Signal Processing, Volume 7, Issue 1, 66-73, 2013.
4. D. Danesin, C. Girardin, A. Sorniotti, A. Morgando, M. Velardocchia, "Driveline layout influence on four-wheel drive dynamics", SAE Transactions, Section 6: Journal of passenger cars: Mechanical systems, Volume 113, 534-541, 2004.
5. C. Chen, T. Ma, H. Jin, Y. Wu, Z. Hou, F. Li, "Torque and rotational speed sensor based on resistance and capacitive grating for rotational shaft of mechanical systems", Mechanical Systems and Signal Processing, Volume 142, 106737, 2020.
6. P. Bingham, S. Theodossiades, T. Saunders, E. Grant, R. Daubney, "A study on automotive drivetrain transient response to 'clutch abuse' events", Proceeding of the Institution of Mechanical Engineers, Part D: Journal of Automobile Engineering, Volume 230, Issue 10, 1403-1416, 2015.
7. J. C. Schnackenberg, "Wheel load transducer", US6439063B1, 2002.
8. N. Werner, "Recorder for measuring applied forces has a rotationally symetric body with measurement legs arranged between through holes on which strain gages are placed to measure shear forced, wgich are insensitive to load placement", DE10055933A1, 2002.
9. M. Grandl, "Torque sensor having a sealing membrance", CN109661566A, 2019.
10. A. Niedworok, "Dynamic Torque Measurement of Drive Transmission in Vehicles Being in Motion Using Strain Gauges Measurement Technique and Wireless Data Transmission", 16th European Conference on Power Electronics and Applications Conference Book,1-8, 2014.
11. T. Sanponpute, C. Watthong, "Prototype of Load Cell Application in Torque Measurement", IMEKO 2010, 285-289, 2010.
12. B. S. H. Tonin, Y. He, N. Ye, H. P. Chew, A. Fok, "Effects of tightening torque on screw stress and formation of implant-abutment microgaps: A finite element analysis", The Journal of Prosthetic Dentistry, 2021.
13. J. Bai, X. Wu, F. Gao, H. Li, "Analysis of powertrain loading dynamic characteristics and the effects on fatigue damage", Applied Sciences, Volume 7, Issue 10,1-15, 2017.
14. R. G. Budynas, J. K. Nisbett, "Shigley's Mechanical Engineering Design_TextBook" Mcgraw-Hill, 2011.
15. L. Mendoza and E. Yuen, "Diseño de un prototipo de máquina trituradora de botellas PET", Peru Technology University, 2019.
16. https://www.ni.com/en-tr/innovations/white-papers/07/measuring-strain-with-strain-gages.html,13/8/21.
17. Y. Chen, "Development of highly magnetostrictive composites for applications in magnetomechanical torque sensors", Iowa State University, 1999.
18. ISO 18265 Metallic materials Conversion of hardness values.
19. https://www.ni.com/en-tr/innovations/white-papers/07/measuring-strain-with-strain-gages.html, 1.8.21.
20. D.M. Ştefănescu, "Wheatstone Bridge - The Basic Circuit for Strain Gauge Force Transducers. In: Handbook of Force Transducers.", Springer, 2011.
21. P. R. Nagarajan, B. George, V. J. Kumar, "A Linearizing Digitizer for Wheatstone Bridge Based Signal Conditioning of Resistive

Sensors", IEEE Sensors Journal, Volume 17, Issue 6, 1696 – 1705, 2017

22. P. Tawadros, M. Awadallah, P. Walker, N. Zhang, "A low-cost bluetooth torque sensor for vehicle jerk and transient torque measurement", Proceedings of the Institution of Mechanical Engineers, Part D: Journal of Automobile Engineering, Volume 234, Issue 2-3, 2020
23. D. Marioli, P. Rolla, A. Taroni, "Strain gauge transducers: an evaluation of accuracy limits", Measurement, Volume 10, Issue 3, 98-104, 1992.
24. DIN 51309 Materials testing machines - Calibration of static torque measuring devices.